

Identification of chemically diverse Chk1 inhibitors by receptor-based virtual screening

Nicolas Foloppe,* Lisa M. Fisher, Rob Howes, Andrew Potter,
Alan G. S. Robertson and Allan E. Surgenor

Vernalis (R&D) Ltd, Granta Park, Abingdon, Cambridge CB1 6GB, UK

Received 17 January 2006; revised 7 March 2006; accepted 14 March 2006

Available online 29 March 2006

Abstract—Inhibition of the Chk1 kinase by small molecules is of great therapeutic interest for oncology and in understanding the cellular regulation of the G2/M checkpoint. We report how computational docking of a large electronic catalogue of compounds to an X-ray structure of the Chk1 ATP-binding site allowed prioritisation of a small subset of these compounds for assay. This led to the discovery of 10 novel Chk1 inhibitors, distributed among nine new and clearly different chemical scaffolds. Several of these scaffolds have promising lead-like properties. All these ligands act by competitive binding to the targeted ATP site. The crystal structures of four of these compounds bound to this site are presented, and reasonable modelled docking modes are suggested for the 5 other scaffolds. This structural context is used to assess the potential of these scaffolds for further medicinal chemistry efforts, suggesting that several of them could be elaborated to make additional interactions with the buried part of the ATP site. Some unusual interactions with the conserved kinase backbone motif are pointed out. The ligand-binding modes are also used to discuss their medicinal chemistry potential with respect to undesirable chemical functionalities, whether these functionalities bind directly to the protein or not. Overall, this work illustrates how virtual screening can identify a diverse set of ligands which bind to the targeted site. The structural models for these ligands in the Chk1 ATP-binding site will facilitate further medicinal chemistry efforts targeting this kinase.

© 2006 Elsevier Ltd. All rights reserved.

1. Introduction

The human Chk1 kinase, which plays an essential role in the regulation of the cell cycle G2/M checkpoint,^{1–10} is a promising target for the development of small molecule inhibitors against cancer.^{11–20} Selective Chk1 inhibitors should also prove useful to study the regulation of the G2/M checkpoint from a fundamental biology point of view.

Only a few chemical classes acting as human Chk1 inhibitors have been reported.^{9,11,15–17,19,21–26} Many of these inhibitors are natural products such as debromohymenialdisine,⁹ staurosporine and its deriva-

tives.^{15–17,21–23} A few drug-like Chk1 inhibitors have been reported,^{11,19,24–27} however, there is clearly a need to identify more such Chk1 inhibitors, given the typical attrition rate in drug discovery.

The available crystal structures of the kinase domain of human Chk1^{18,25,28,40} can be used to perform computational screens of electronic compound libraries, with the aim of finding new ligands binding to the ATP-binding site. In this approach, small molecules are computationally docked into the three-dimensional structure of the target site.^{29–32} The overall orientation of the small molecule, as well as its intramolecular conformations, are explored and the interactions between receptor and putative ligand scored³³ for each configuration. This allows ranking of libraries of existing compounds according to their calculated interaction scores and prioritisation of the compounds for experimental assays. This virtual screening (VS) strategy has met with increasing success.^{19,29–31,34–37} This approach has recently yielded new Chk1 inhibitors with sub-micromolar affinity, although not all of them have been disclosed.¹⁹

Abbreviations: HTS, experimental high-throughput screening; PDB, Protein Data Bank; SAR, structure–activity relationship; VS, virtual screening.

Keywords: Docking; Drug design; Oncology; Virtual screening; X-ray crystallography.

* Corresponding author. Tel.: + 44 0 1223 895 338; fax: + 44 0 1223 895 556; e-mail: n.foloppe@vernalis.com

We report here how high-throughput docking of a large electronic catalogue of commercially available compounds^{38,39} led us to identify chemically diverse scaffolds which inhibit human Chk1 with affinities in the micromolar range. These scaffolds are novel as Chk1 inhibitors. The mode of action of these inhibitors was determined by traditional enzyme kinetic methods; all of them were found to be ATP competitive. For some of the inhibitors this was confirmed by the X-ray structure of the ligand bound to the Chk1 ATP site. When an X-ray structure of the bound ligand could not be obtained, a tentative reasonable docking mode is suggested. This structural context is used to evaluate the potential of these new Chk1 inhibitors for further elaboration. In particular, several of these new scaffolds could be derivatised towards a buried pocket of special interest to gain potency and selectivity when designing ligands targeting Chk1.^{25,40} Also, the binding modes are used to discuss the possible replacement of chemical functionalities which are perceived as undesirable for medicinal chemistry, further illustrating the value of obtaining structural information before embarking on lead optimisation.

2. Results and discussion

2.1. Discovery of 9 new scaffolds for ATP competitive inhibition of Chk1

Both theoretical⁴¹ and empirical⁴² arguments suggest that lead compounds should be of relative limited complexity. In view of these arguments, computational filters were first applied to the in-house electronic catalogue of commercially available compounds,^{38,39} such that only compounds with less than six rotatable bonds and molecular weight between 250 and 550 were kept for docking. Application of these filters is also expected to enrich the docking library with compounds having favourable absorption properties⁴³ and for which the conformational search during docking should be relatively efficient. Compounds with reactive chemical functionalities which could obscure the readout of an *in vitro* binding assay were also removed.^{39,44,45} However, other chemical functionalities with possible *in vivo* metabolic liabilities were not discarded at this early stage, given the possibility that they could be removed or replaced during subsequent optimisation of the compounds. This resulted in a set of ~700,000 compounds which were docked with the program rDock^{31,46,47} into an X-ray structure of the Chk1 ATP-binding site.²⁸ The screen was set up such that only the compounds which achieved at least a predefined intermolecular score threshold were kept for further analysis, yielding ~15,000 unique compounds. These were ranked based on their intermolecular docking scores, and the docking modes of the best ranking 2000 compounds (set A) were inspected visually. Set B was comprised of the ~13,000 remaining compounds. Visual inspection of compounds in set A was performed to discard docking modes deemed unlikely to lead to real binding, for instance when large voids were present between ligand and protein, or when the docking pose buried ligand charged

groups in a hydrophobic pocket of the targeted site. After this filtering only 480 compounds remained in set A. A diverse subset of 1000 compounds was extracted from set B, based on the two-dimensional MACCS fingerprints as implemented in the program MOE,⁴⁸ and a Tanimoto similarity coefficient adjusted to select this number of compounds. This yielded a final list of 1480 prioritised compounds, and 1179 of them were subsequently obtained and assayed.

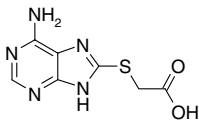
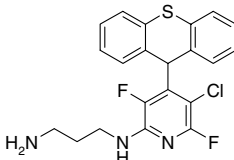
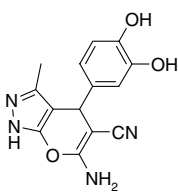
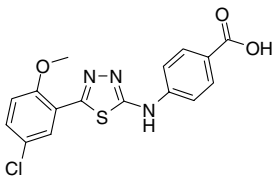
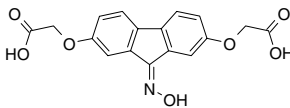
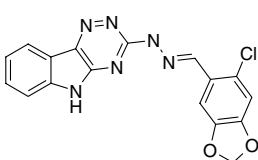
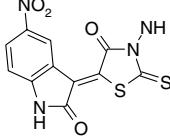
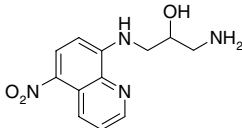
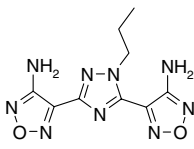
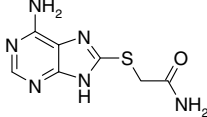
The active Chk1 inhibitors were the compounds showing $\geq 50\%$ inhibition in the Chk1 kinase assay at a compound concentration of 50 μM or less. These compounds were subjected to IC_{50} determinations and quality control, leading to nine confirmed active inhibitors (compounds 1–9, Table 1), that is ~0.8% of the number of assayed compounds.

Compound 10 was also identified to be a Chk1 inhibitor, by its close analogy with compound 1. Analysis of the mechanism of Chk1 inhibition by traditional enzymatic kinetic methods indicated that compounds 1–10 act by competing with ATP for its binding site. This was confirmed directly by X-ray crystallography for four of the inhibitors (see below). It is interesting to note that compounds 1, 2, 3, 4, 6 and 7 were selected as part of set A (see above) after visual inspection of the docking poses. Only compounds 5, 8 and 9 were part of the larger set B extracted with a diversity analysis. Therefore, a hit rate of 1.2% would have been achieved if only the hand-picked compounds (set A) had been assayed.

Compounds 1–9 have very different chemical scaffolds and arguably represent a diverse set of compounds. Therefore, this report illustrates how a receptor-based virtual screening, which does not rely on any particular initial chemotype, can identify several new and very different ligands. It would probably be more difficult to obtain such chemical diversity with ligand-based virtual screening strategies, which are typically informed by commonalities across an initial set of known active ligands.^{49–52} It is well known that having several different starting scaffolds is strongly recommended for drug discovery efforts, given the typically high attrition rate during this process.

Our overall success rate of 0.8% appears modest when compared to a ~35% hit rate (36 hits out of 103 assayed compounds) achieved in a previous virtual screen against Chk1.¹⁹ Several factors could explain this large difference, including differences in the compound libraries used for the two virtual screens. The much higher hit rate obtained by Lyne et al. probably results from their pre-screening of the compound library with a pharmacophoric query, to keep for docking only compounds capable of two-pronged hydrogen bonds with the kinase backbone motif, typically observed in ligand–kinase complexes.⁵³ The formation of these hydrogen bonds was subsequently enforced during docking, yielding a more plausible output. However, the 36 Chk1 inhibitors identified with this protocol corresponded to 4 chemical classes only. This suggests that performing a virtual screen with empirical restraints favouring a hydrogen-bond pattern commonly found in ligand–kinase

Table 1. Structures of compounds **1–10** and their binding affinities to Chk1

Compound	Structure	IC ₅₀ ^a (μM) (SD)
1		31.8 (5.6)
2		15.8 (9.6)
3		20.4 (2.5)
4		26.6 (5.0)
5		13.4 (1.5)
6		20.1 (6.1)
7		72.7 (37.8)
8		27.3 (3.0)
9		17.3 (2.9)
10		15.6 (3.9)

^a Every reported IC₅₀ is the average of at least two measurements, with standard deviations given in parenthesis.

complexes is an efficient way to increase the hit rate; that may, however, inherently limit the chemical diversity of the hits. This interpretation is supported by a study which compared the outcomes of experimental

high-throughput screening (HTS) and VS (docking) against the GSK-3β kinase, using a same library of compounds.⁵⁴ This work also compared a variety of VS protocols, with and without pharmacophoric

restraints. The hit rate from the HTS was 0.55%, and 12.9% from the most productive VS protocol (with pharmacophoric restraints). An interesting observation was that the VS identified only 4 of the 6 chemical classes of hits found in the HTS. Analysis of the docking protocol indicated that the pharmacophoric restraints played a role in excluding compounds belonging to two chemical classes missed by the VS, because they did not meet the pharmacophoric criteria. Our results illustrate how this can happen when considering the two-point pharmacophore condition used by Lyne et al. with Chk1, which required two hydrogen bonds between ligand and (i) the backbone NH of Cys87 and (ii) the backbone carbonyl of Glu85. Compound **8** (Fig. 1) would not meet this condition. Compound **10** meets this condition in reality (Fig. 1), but may not during a VS if the scoring function does not recognise polarised C–H groups as hydrogen-bond donors.^{55,56} The hit rate of 0.55% in the HTS from Polgár et al. falls in the 0.15–0.64% success rate reported for a random set of compounds screened against undisclosed kinases.⁵⁷ This suggests that our VS may have performed only slightly

better than random screening, although no convincing conclusion can be drawn in that respect because hit rates depend on: (i) the target, (ii) the compounds screened and (iii) the definition of a hit. Importantly, our VS screen yielded new and diverse starting points for medicinal chemistry.

Some of the compounds shown in Table 1 are a priori more attractive than others as starting points for medicinal chemistry efforts. For example, compounds **5** and **9** may not seem very promising because their high degree of symmetry, combined with a lack of functionalities amenable to derivatisation, severely limits the possibilities for further elaboration. The marked lipophilic character of compounds **2** and **6** (calculated $\log P^{58}$ of 3.4 and 6.0, respectively) may also hinder their progression.⁴³ To put this in context, however, UCN01 (to our knowledge the only Chk1 inhibitor currently in clinical trials^{13,14}) is also a bulky lipophilic compound (calculated $\log P = 4.3$). The smaller compounds **1**, **3**, **4**, **7**, **8** and **10** are more lead-like^{41,42} despite possible issues with some chemical functionalities such as catechol

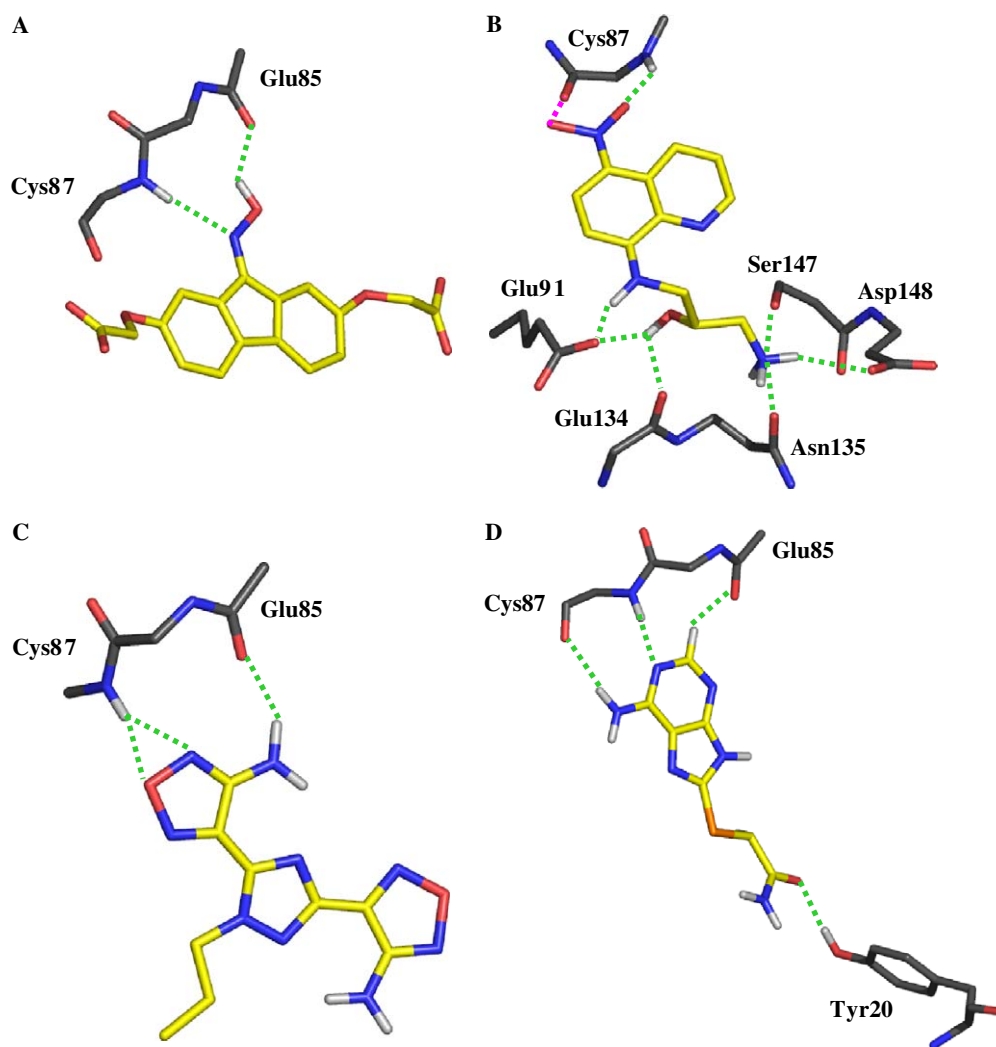


Figure 1. Crystallographic-binding mode of compounds **5**, **8**, **9** and **10** in the ATP-binding site of Chk1, in panels A, B, C and D, respectively. For clarity, only selected residues and hydrogen atoms are shown. Glu85 and Cys87 are part of the conserved kinase backbone binding motif. Hydrogen bonds between the compounds and the kinase are depicted with green dotted lines. In panel B, a contact (distance = 3.1 Å) between a nitro oxygen of compound **8** and the carbonyl oxygen of Cys87 is depicted with a magenta dotted line.

in **3**, hydrazine in **7** and nitro in **8**, which are frequently perceived as undesirable due to their lack of metabolic stability and possible association with toxicity.^{59–61} This is also a concern with the hydrazone in **6**.⁶¹ Compounds **1**, **4** and **10** are devoid of such liabilities. Importantly, the potential for modification or replacement of every chemical functionality in compounds **1–10** can be assessed in a structural context provided either by X-ray crystallography or computational modelling.

2.2. X-ray-binding modes

X-ray crystallography was attempted for all 10 compounds but crystal structures could only be obtained for 4 of them (Table 2, Fig. 1). An X-ray structure was obtained for Chk1 complexed to compound **10**, which is fortunate because this compound has very favourable lead-like attributes,^{41,42} such as a small size with scope for further elaboration. The purine of **10** hydrogen-bonds the highly conserved backbone kinase motif at the hinge between the two lobes of the kinase domain (Fig. 1A). Hydrogen bonds to this motif are observed with almost all other kinase inhibitors^{53,62,63} and that is again illustrated in the present work. The amide of **10** is hydrogen-bonded to Tyr20, which is part of a solvent exposed loop at the periphery of the ATP-binding site. This loop segment was poorly defined in some analogous X-ray structures of the Chk1 kinase domain^{25,28} and it is expected that this flexible part of the protein could adjust in response to a variety of substituents that could substitute the amide. The tautomer suggested in Figure 1D for the imidazole of **10** is arbitrary, however, the corresponding N–H vector points to an area of the binding site where derivatisation would allow extensive interactions between the added buried substituents and the binding site. Therefore, the structural context shows that there is scope for further elaboration of **10** towards improved potency.

An X-ray structure was also obtained for compound **8** bound to the Chk1 ATP-binding site (Fig. 1B). Compound **8** is a synthetically tractable scaffold with lead-like properties, with the possible exception of its nitro group; it is known that such groups have potential metabolic and toxic liabilities^{60,61} although a nitro group is present in some used drugs (e.g., nitrofurazone⁶¹ or chloramphenicol⁶⁵) and in a significant fraction of the compounds tested in human clinical trials.⁴⁴ The nitro group of **8** is buried in the ATP-binding site, where one of its oxygens forms a hydrogen bond with Cys87 of the conserved kinase backbone motif. Interestingly, the other oxygen of this nitro group is in direct contact with the carbonyl oxygen of Cys87 (oxygen–oxygen distance of 3.1 Å), which is presumably unfavourable energetically. This highlights the need for sub-optimal protein–ligand interactions to be tolerated to some degree in virtual screening scoring functions at the initial stage of the discovery process, as illustrated in another recent report.²⁵ This may complicate the use of automated filters developed to process the output of virtual screening.⁶⁶ One benefit of the crystal structure is to show that the nitro group is intimately involved in the ligand–protein interactions and not in a peripheral position where it could be easily replaced (such as with **7**, see below). The potential of **8** for further medicinal chemistry should be seen in this context. The X-ray structure also clearly shows that it is the S stereoisomer of the aliphatic chain of **8** which binds to Chk1, with the ligand hydroxyl group forming a bifurcated hydrogen bond with the carboxylate of Glu91 and the backbone carbonyl oxygen of Glu134. The primary amino group of **8** hydrogen-bonds with Asn135 and Ser147. The pyridine moiety of **8** is well positioned for further substitutions which could interact extensively with buried areas of the binding site, potentially leading to dramatic improvements in potency.

Table 2. Crystallographic data collection and refinement statistics for Chk1 in complex with compounds **5**, **8**, **9** and **10**

Structure	Chk1 + compound			
	5	8	9	10
<i>Data collection statistics</i>				
Resolution (Å)	2.50	2.60	2.20	2.20
Measured reflections	124644	182585	125958	132947
Unique reflections	11961	10278	17692	17851
Completeness: overall/in hrb ^a (%)	70.5/22.1	79.9/36.0	96.1/79.1	98.2/51.2
Average multiplicity/in hrb	4.1/0.9	1.9/0.8	3.8/1.1	4.3/1.3
Mean <i>I</i> /σ <i>I</i> : overall/in hrb	10.6/2.3	9.2/2.2	17.5/2.9	15.2/2.7
<i>R</i> _{merge} : overall/in hrb (%)	8.4/22.6	10.0/28.7	6.0/27.3	5.1/30.4
<i>Refinement statistics</i>				
<i>R</i> _{free} (%)	27.1	25.6	24.9	25.8
<i>R</i> _{cryst} (%)	18.1	17.9	18.6	18.8
Rms deviations				
Bonds (Å)	0.021	0.031	0.018	0.024
Angles (°)	2.059	2.728	1.837	2.102
<i>B</i> Factor (Å ²)	2.60	3.51	2.63	3.21
PDB code ^b	2CGU	2CGV	2CGW	2CGX

*R*_{free} is the *R* factor calculated using 5% of the reflection data chosen randomly and omitted from the refinement process, whereas *R*_{cryst} is calculated with the remaining data used in the refinement. Rms bond lengths and angles are the deviations from ideal values; the rms deviation in *B* factors is calculated between covalently bonded atoms.

^a hrb, highest resolution bin.

^b Protein Data Bank entry codes.

The binding modes of compounds **5** and **9** in the Chk1 ATP site were also ascertained by crystallography. Compound **5** hydrogen-bonds to the conserved kinase backbone motif via an oxime functionality (Fig. 1A), which is arguably unusual, and possibly new, in terms of kinase inhibitors.^{53,62,67,68} The hydroxyl part of the oxime donates a hydrogen bond to the carbonyl oxygen of Glu85, while the imino nitrogen accepts a hydrogen bond from the amide nitrogen of Cys87. Unfortunately, the largely symmetric nature of **5** is not particularly attractive for further medicinal chemistry efforts, although the crystal structure would allow a smaller scaffold comprised of a substructure of **5** to be designed for further elaboration. The same type of remarks hold for **9**, which hydrogen-bonds to the kinase backbone motif via one of its oxadiazole rings and a pendant amino group (Fig. 1C). From a structural point of view, the second oxadiazole ring of **9** is in an interesting position to access other parts of the binding site, but the chemical nature of this ring prevents further substitutions in those directions. Thus, one could design an analogue of **9** where this second oxadiazole ring would be replaced by a more suitable moiety.

In sum, the X-ray structures presented here revealed some interesting intermolecular interactions regarding the chemical functionalities found to hydrogen-bond the conserved kinase backbone motif. Some of these interactions are arguably unusual, and possibly new, in the context of the medicinal chemistry of kinase inhibitors. Maybe more importantly, this firm structural context helps to assess the potential of an inhibitor for further medicinal chemistry efforts. That holds even for scaffolds of apparent limited interest, because one may glean useful information about the binding mode of substructures of these scaffolds.

2.3. Computational docking models

Crystallisation studies were attempted for all inhibitors obtained from the virtual screening, however, no experimental structure could be obtained for Chk1 in complex with compounds **1**, **2**, **3**, **4**, **6** and **7**. Given the clear usefulness of assessing a ligand scaffold when bound to its target, an alternative is to consider docking modes generated solely by computational means. Such docking modes are not meant to replace X-ray structures but to provide working hypotheses to guide further experimental work, following which the initial hypotheses may be adjusted. The best scoring docking modes for **2**, **3**, **4**, **6** and **7** obtained with software rDock are shown in Figure 2. These docking modes should only be regarded as suggestions in need of experimental testing, given that even convincing docking models may be inaccurate.²⁵ A significant fraction of docking models, however, is typically in reasonable agreement with experimental data.^{69–73} We have presented an example with Chk1 where such models were predictive and useful.⁴⁰ Predictions are facilitated with ligands binding to kinase ATP sites, given that the aromatic core of these ligands tends to bind in the same plane as the native adenine moiety, and typically forms recurrent hydrogen bonds with the conserved kinase backbone motif.^{53,62,68}

The proposed docking modes for **2**, **3**, **4**, **6** and **7** follow this pattern (Fig. 2).

Before examining docking modes of compounds **2**, **3**, **4**, **6** and **7**, we briefly comment on those obtained for compounds **5**, **8**, **9** and **10**, for which the experimental solution is known (Fig. 1). This does not provide a statistically valid assessment of the chance of success when predicting a binding mode with the program rDock, but it allows to re-iterate common arguments to keep in mind when considering docking modes generated with an empirical scoring function and a fixed receptor. Docking modes similar (overall orientation and key interactions with the ATP site) to their experimental counterpart were among the top 12 best ranked solutions for **5**, **8**, **9** and **10**. This is already a degree of success, but the difficulty would have been to recognise the correct solution when other reasonable suggestions were offered. For **8** it would have been exceedingly difficult to identify the experimental binding mode from the computational suggestions, maybe because of a subjective reluctance to accept the interaction between a nitro group and the kinase motif. Also, the docking poses did not help to discriminate *a priori* between the R and S stereoisomers of **8** in terms of binding mode. Docking of **10** must take into account two possible tautomers regarding the position of the proton on the imidazole nitrogens. This leads to a variety of reasonable docking modes with different ligand overall orientations, but for which the ligand–protein interaction scores did not differ significantly. This is because the purine of **10** can hydrogen-bond the kinase motif in several ways, and the relative lack of substituents around this core does not help much in identifying a most likely binding mode. The interaction between the amide substituent of **10** and Tyr20 could not be predicted by docking to a rigid receptor because it requires a motion of the loop containing Tyr20. Therefore, we would not have discriminated between the correct and artefactual docking modes of **10**. With **5** and **9**, the correct binding modes were also those which scored best, and the few alternative docking modes were clearly less convincing than these top-ranked solutions in terms of interactions with the protein. Therefore, we would have predicted correctly the binding modes of **5** and **9**. This exercise illustrates the usual pitfalls associated with the prediction of ligand binding modes: alternative tautomers and stereoisomers, unusual protein–ligand interactions, multiple reasonable docking modes, possible conformational changes in the receptor and the neglect of potential water-mediated ligand–protein interactions. Therefore, these computational models are no substitute for a good-quality X-ray structure. However, such modelling frequently suggests helpful binding modes, which can be used to generate ideas for further synthetic efforts. This is what is attempted in the following for compounds for **2**, **3**, **4**, **6** and **7**.

The nitrogens in the amino-pyridine of **2** constitute a donor–acceptor motif which could be thought to complement precisely the counterpart hydrogen-bonding groups in the conserved kinase motif. However, exhaustive automated docking did not present any binding mode of **2** where it interacts with the kinase backbone motif via its amino-pyridine moiety. Manual modelling

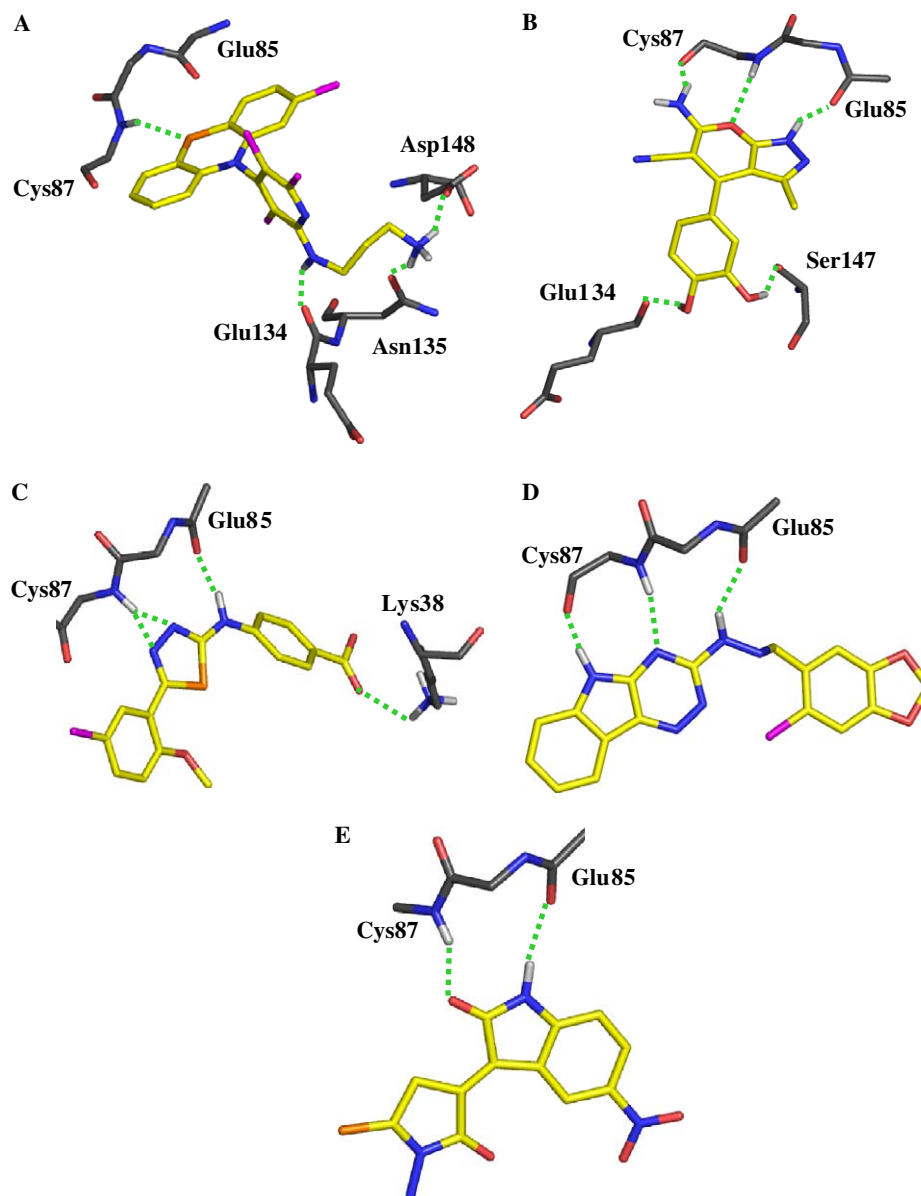


Figure 2. Possible docking modes of compounds **2**, **3**, **4**, **6** and **7** in the ATP-binding site of Chk1, in panels A, B, C, D and E, respectively. For clarity, only selected residues and hydrogen atoms are shown. Glu85 and Cys87 are part of the conserved kinase backbone binding motif. Hydrogen bonds between the compounds and the kinase are depicted with green dotted lines.

of such binding mode (ligand pyridine and amino nitrogens accepting and donating a hydrogen bond from and to the Cys87 backbone N–H and carbonyl, respectively) reveals it would entail very severe steric clashes between the tricyclic moiety of **2** and the protein at the periphery of the ATP-binding site, for instance with Leu15, Gly16 and Ser147. This is because due to intramolecular steric contacts, the tricyclic system is quasi-perpendicular to the plane of the pyridine ring of **2**. Therefore, such a binding mode would require rather dramatic conformational changes regarding the overall opening of the ATP-binding cleft. This cannot be excluded, but the docking mode presented in Figure 2A is also reasonable because it buries the maximum amount of ligand apolar surface area, a well-known driving force of protein–ligand association.^{74,75} In this docking mode, the tricyclic apolar moiety is buried in the ATP-binding site with

van der Waals contacts to Leu15, Val23, Ala36 and Leu137 (not shown), and its sulfur forming a weak hydrogen bond with the amide of Cys87 (Fig. 2A). The limited role of hydrogen bonds between ligands and the kinase motif in driving potency has already been noted.^{25,74} A weak N–H...S hydrogen bond would be reminiscent of the weak C–H...O hydrogen bonds frequently observed in ligand–kinase complexes.⁵⁶ A hydrogen bond could be formed between the aromatic amino group and the backbone carbonyl oxygen of Glu134. The primary amine of **2** could occupy a position reminiscent of that observed by X-ray crystallography for **8** (Fig. 1B), with hydrogen bonds to the side chains of Asn135 and Asp148. In absence of crystal structure, an obvious strategy to make progress with compound **2** would be to separate the pyridine and tricyclic parts of the compound, and investigate binding of these two

substructures separately. This would be expected to identify the substructure which interacts directly with the kinase motif, assuming that the other substructure would not bind alone.

The docking mode of **3** (Fig. 2B) was obtained with the S stereoisomer. Another sensible docking mode, although it scored slightly less favourably, can also be found with the R stereoisomer, with the compound bicyclic core flipped relative to the kinase backbone motif and the pyrazole moiety hydrogen-bonding Cys87 instead of Glu85. In both of these docking modes, the π face of the catechol packs closely against Leu137 (not shown), with the hydroxyl groups hydrogen-bonding the backbone carbonyl oxygen of Glu134 and the side chain of Ser147. If the role of these hydrogen bonds for the binding of **3** to Chk1 were confirmed, this could prove a liability for this scaffold, given the propensity of catechols to be quickly glucuronidated, which would lead to inactivation of the scaffold. However, the catechol is solvent exposed and at the periphery of the binding site in this docking model, therefore it is possible that the catechol could be replaced altogether, with other substituents grafted onto the buried bicyclic scaffold directly hydrogen-bonded to the kinase motif.

Compound **4** is a synthetically tractable lead-like scaffold with no chemical functionalities having a priori potential metabolic or toxicity liabilities. In its preferred docking mode (Fig. 2C), compound **4** hydrogen-bonds the kinase motif via its amino-thiadiazole core. Its carboxylate forms an ionic pair with Lys38. This ionic interaction seems to favour this docking mode over an alternative which would be flipped relative to the kinase motif, with the compound amino group hydrogen-bonding Cys87 instead of Glu85. Of course, this alternative binding is still a very real possibility. In the docking mode of Figure 2C, the benzoic acid moiety is favourably positioned for further derivatisation towards buried regions of the binding site, including a pocket of special interest in the vicinity of Asn59^{25,40} (Fig. 3).

The docking mode of compound **6** also suggests that its fused tricyclic scaffold may be of great interest to reach to this pocket. The tricyclic moiety forms three standard hydrogen bonds with the backbone of Cys87 and Glu85 of the kinase motif (Fig. 2D). Again, the binding mode of this core could be flipped with respect to the kinase motif, with the chloro-benzodioxole substituent being solvent accessible. The best-scoring docking mode, however, buries the chloro-benzodioxole substituent such that it contacts Lys38, Asn59, Leu84 and Asp148 (not shown). Many of these contacts, however, appear suboptimal and therefore a possible strategy would be to replace the chloro-benzodioxole altogether. This would be combined with the replacement of the undesirable hydrazine moiety by an amino linkage. This amino linkage would be in a favourable position for derivatisation to access the pocket of particular interest around Asn59 (Fig. 3).

The undesirable hydrazine and nitro groups in **7** may also be replaced while keeping the remainder of the scaffold,

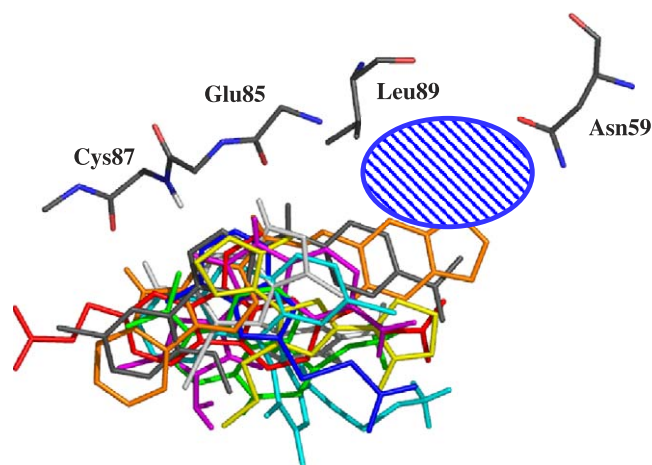


Figure 3. Superposition of the structures of the Chk1 ATP site in complex with compounds **2–10**. The conserved hinge backbone of the kinase motif, to which compounds are hydrogen bonded, was closely aligned across all proteins and only one representative structure of this backbone is shown for simplicity. Every compound is in a different colour. This overlay shows that this diverse set of ligands interacts with various areas of the binding site. For compounds **5**, **8**, **9** and **10** the structures were obtained by X-ray crystallography (Fig. 1), while for compounds **2**, **3**, **4**, **6** and **7** the structures are the docking models shown in Figure 2. The blue striated oval marks the location of a buried pocket which was shown to be of special interest to gain potency and selectivity against Chk1.^{25,40} Several of the newly discovered ligand scaffolds would be favourably positioned to reach into this pocket.

fold, given that these groups face towards the solvent in the docking mode shown in Figure 2E. In addition, the phenyl ring of **7** is favourably positioned to access the pocket of special interest around Asn59. Therefore, **7** should be considered as an interesting starting point for further elaboration.

Overall, reasonable docking models in the Chk1 ATP site can be obtained for compounds **2**, **3**, **4**, **6** and **7**, consistent with their ATP competitive mechanism of inhibition. These docking modes reflect the generally observed features of the binding modes of kinase inhibitors, but should be regarded as working hypotheses only. In particular, alternative docking modes can be found where the ligand moiety hydrogen-bonding the kinase backbone motif can be flipped relative to this motif. It remains that the presented docking modes allow the formulation of specific working hypotheses to further elaborate these ligands towards improved potency and selectivity for Chk1.

Figure 3 presents an overlay of all binding modes shown in Figures 1 and 2. This indicates that these diverse scaffolds interact with different parts of the binding site. This could provide ideas to transfer elements from one ligand to another, and to other known Chk1 inhibitors. Figure 3 also shows that ligands **1–10** do not take advantage of a buried pocket around Asn59, which could be used to gain potency and selectivity when targeting Chk1. As mentioned above, some of the scaffolds presented here are expected to open new opportunities to target this pocket.

3. Conclusions

Ten new ligands of the Chk1 kinase were discovered by docking a large electronic catalogue of compounds to its ATP-binding site, and by assaying a relatively small number of prioritised compounds. These compounds inhibit Chk1 in an ATP competitive manner and have affinities for Chk1 in the low micromolar range. Importantly from a medicinal chemistry point of view, these ligands are chemically diverse and therefore offer a variety of potential starting points for further elaboration. Compounds **1**, **4** and **10** are arguably of particular interest because of their lead-like properties, including a relatively small size, well-balanced physico-chemical properties and the absence of chemical functionality associated with metabolic or toxic liability.

The medicinal chemistry potential of each newly disclosed chemical scaffold is discussed in the context of its binding modes to the protein, either determined by X-ray crystallography or modelled computationally. X-ray-binding modes were obtained for compounds **5**, **8**, **9** and **10**. This information could be exploited to devise synthetic efforts directly on the more interesting compounds **8** and **10**, or around substructures of the symmetric scaffolds of **5** and **9**. These X-ray structures also reveal interesting interactions between the kinase conserved motif and ligand functionalities that it contacts directly.

In addition, docking modes were generated for compounds **2**, **3**, **4**, **6** and **7**. The presented docking modes display the features typically associated with ligands bound to kinase ATP-binding sites, and are therefore reasonable working hypotheses. These structural models are helpful in providing concrete starting points to inform further ligand design, but we re-iterate that these models are not as reliable as experimental X-ray structures, and should therefore be interpreted as such. However, only a limited number of alternative sensible docking modes could be found for each of these scaffolds, which suggests that structure-based ligand design is a realistic prospect for several of these ligands. In particular, several of these scaffolds are likely to be well positioned to access a pocket of special interest in the vicinity of Asn59 to gain potency and selectivity when targeting the Chk1 kinase.^{25,40}

4. Computational and experimental methods

4.1. Computational screening

The preparation of the screened electronic catalogue of commercially available compounds has been presented elsewhere.^{38,39} Filtering of the catalogue of compounds on molecular weight ($250 \leq MW \leq 550$) and number of rotatable bonds ($NRot \leq 6$) to prepare the set of compounds used for docking was performed with in-house perl scripts, and left ~700,000 compounds for subsequent screening. The initial three-dimensional

structure of these compounds was then generated with CORINA,⁷⁶ with removal of counterions or solvent fragments, all chemical functionalities in their neutral state and generation of multiple ring conformations within 7 kJ/mol of the lowest energy ring conformation. Only one stereoisomer and tautomer per compound was generated with CORINA for the computational high-throughput screen.

Computational screening was performed by docking the three-dimensional structure of each compound to the ATP-binding site of the crystal structure of apo human Chk1 (PDB⁷⁷ entry 1IA8²⁸). Water molecules were removed from the coordinates and polar hydrogens added to the protein using the CHARMM force-field.⁷⁸ To specify the docking volume, the ATP-bound crystal structure of protein kinase A (PDB entry 1ATP) was superimposed onto that of Chk1. There was unambiguous superimposition of the ATP-binding sites and the docking volume in Chk1 was defined as the space within 8 Å of the ATP molecule. Docking was performed with the program rDock which is an extension of the program RiboDock,⁴⁶ using an empirical scoring function calibrated based on protein–ligand complexes.^{31,47}

Docking was carried out on a PC cluster of 100 CPUs. Acidic functionalities were deprotonated, basic functionalities protonated and apolar hydrogens removed with rDock. The Monte Carlo/simulated annealing protocol initially used in RiboDock⁴⁶ was replaced by a steady state Genetic Algorithm (GA) to improve the efficiency of the docking search. Ligand docking poses were represented using a conventional chromosome representation of translation, rotation and rotatable bond dihedral angles. A single GA population was used, of size proportional to the number of ligand rotatable bonds, with a mutation:crossover ratio of 3:2. The overall orientation and internal conformation of the compounds were searched with the GA, while the protein was kept fixed.

The docking modes of the confirmed hits were investigated in more detail with the same fixed protein structure as used during the computational high-throughput screen. All reasonable combinations of stereoisomers and tautomers were considered when investigating in more detail the docking modes of the newly discovered inhibitors. Those were built manually with MOE, which was possible given the relatively small number of combinations. These compounds were energy-minimised with the Merck molecular force-field⁷⁹ before regenerating their docking modes with more exhaustive docking. It was performed with 200 docking runs per stereoisomer/tautomer. The resulting 200 docking poses were ranked based on the docking scores and inspected visually.

4.2. Kinase assays for IC₅₀ determinations

Enzyme inhibition assays to determine IC₅₀s with human Chk1 were performed as described previously.^{25,40}

4.3. Crystallisation and three-dimensional structure determination

Chk1 1–289 construct was expressed, purified and crystallised as previously described.²⁵ Obtention and analysis of X-ray diffraction data, as well as protocols to build and refine the crystal structures of the protein–ligand complexes, were also as previously described.^{25,40} Full data collection and refinement statistics are presented in Table 2.

4.4. Compound suppliers and quality control

The active compounds were purchased from the following sources: **1**, **3**, **8** and **10** from Asinex⁸⁰; **2**, **4** and **9** from InterBioScreen⁸¹; **5** from ChemDiv⁸²; **6** and **7** from Chembridge.⁸³

Every compound which inhibited Chk1 in the kinase IC₅₀ assay was subjected to a liquid chromatography–mass spectrometry (LC–MS) analysis, and the chemical structures given in Table 1 were consistent with the masses obtained by MS, to a purity of at least 85%. Purity was assessed by UV detection at three wavelengths and total ion current under positive ion electrospray.

Acknowledgements

We thank the support staff of SBC-19ID at the Advanced Photon Source (Argonne, Chicago) for help with data collection. We also thank Drs. I-Jen Chen and Christine Richardson for helpful discussions.

References and notes

- Sanchez, Y.; Wong, C.; Thoma, R. S.; Richman, R.; Wu, Z., et al. *Science* **1977**, *277*, 1497–1501.
- Melo, J.; Toczyski, D. *Curr. Opin. Cell Biol.* **2002**, *14*, 237–245.
- Rhind, N.; Russell, P. *J. Cell Sci.* **2000**, *113*, 3889–3896.
- Chen, Z.; Xiao, Z.; Chen, J.; Ng, S.-C.; Sowin, T., et al. *Mol. Cancer Ther.* **2003**, *2*, 543–548.
- Liu, Q.; Guntuku, S.; Cui, X. S.; Matsuoka, S.; Cortez, D., et al. *Genes Dev.* **2000**, *14*, 2448–2459.
- Zachos, G.; Rainey, M. D.; Gillespie, D. A. F. *EMBO J.* **2003**, *22*, 713–723.
- Luo, Y.; Rockow-Magone, S. K.; Kroeger, P. E.; Frost, L.; Chen, Z., et al. *Neoplasia* **2001**, *3*, 411–419.
- Lopez-Girona, A.; Tanaka, K.; Chen, X.-B.; Baber, B. A.; McGowan, C. H., et al. *Proc. Natl. Acad. Sci. U.S.A.* **2001**, *98*, 11289–11294.
- Curman, D.; Cinel, B.; Williams, D. E.; Rundle, N.; Block, W. D., et al. *J. Biol. Chem.* **2001**, *276*, 17914–17919.
- Furnari, B.; Rhind, N.; Russell, P. *Science* **1997**, *277*, 1495–1497.
- Li, Q.; Zhu, G.-D. *Curr. Top. Med. Chem.* **2002**, *2*, 939–971.
- Tenzer, A.; Pruschy, M. *Curr. Med. Chem.* **2003**, *3*, 35–46.
- Sausville, E. A.; Arbuck, S. G.; Messmann, R.; Headlee, D.; Lush, R. D., et al. *J. Clin. Oncol.* **2001**, *19*, 2319–2333.
- Senderowicz, A. M. *The Oncologist* **2002**, *7*, 12–19.
- Graves, P. R.; Yu, L.; Schwarz, J. K.; Gales, J.; Sausville, E. A., et al. *J. Biol. Chem.* **2000**, *275*, 5600–5605.
- Busby, E. C.; Leistriz, D. F.; Abraham, R. T.; Karnitz, L. M.; Sarkaria, J. N. *Cancer Res.* **2000**, *60*, 2108–2112.
- Jackson, J. R.; Gilmartin, A.; Imburgia, C.; Winkler, J. D.; Marshall, L. A., et al. *Cancer Res.* **2000**, *60*, 566–572.
- Zhao, B.; Bower, M. J.; McDevitt, P. J.; Zhao, H.; Davis, S. T., et al. *J. Biol. Chem.* **2002**, *277*, 46609.
- Lyne, P. D.; Kenny, P. W.; Cosgrove, D. A.; Deng, C.; Zabudoff, S., et al. *J. Med. Chem.* **2004**, *47*, 1962–1968.
- Kawabe, T. *Mol. Cancer Ther.* **2004**, *3*, 513–519.
- Eastman, A.; Kohn, E. A.; Brown, M. K.; Rathman, J.; Livingstone, M., et al. *Mol. Cancer Ther.* **2002**, *1*, 1067–1078.
- Roberge, M.; Berlinck, R. G. S.; Xu, L.; Anderson, H. J.; Lim, L. Y., et al. *Cancer Res.* **1998**, *58*, 5701–5706.
- Kohn, E. A.; Yoo, C. J.; Eastman, A. *Cancer Res.* **2003**, *63*, 31–35.
- Kania, R. S.; Bender, S. L.; Borchardt, A.; Braganza, J. F.; Cripps, S. J. et al. Patent WO 0102369, 2001.
- Foloppe, N.; Fisher, L. M.; Howes, R.; Kierstan, P.; Potter, A., et al. *J. Med. Chem.* **2005**, *48*, 4332–4345.
- Wang, G.; Li, G.; Mantel, R. A.; Chen, Z.; Kovar, P., et al. *J. Med. Chem.* **2005**, *48*, 3118–3121.
- Lin, N.-H.; Xia, P.; Kovar, P.; Park, C.; Chen, Z., et al. *Bioorg. Med. Chem. Lett.* **2006**, *16*, 421–426.
- Chen, P.; Luo, C.; Deng, Y.; Ryan, K.; Register, J., et al. *Cell* **2000**, *100*, 681–692.
- Schneider, G.; Böhm, H. J. *Drug Discovery Today* **2002**, *7*, 64–70.
- Abagayan, R.; Totrov, M. *Curr. Opin. Chem. Biol.* **2001**, *5*, 375–382.
- Barril, X.; Hubbard, R. E.; Morley, D. *Mini-Rev. Med. Chem.* **2004**, *4*, 779–791.
- Kitchen, D. B.; Decornez, H.; Furr, J. R.; Bajorath, J. *Nat. Rev. Drug Discovery* **2004**, *3*, 935–949.
- Böhm, H. J.; Stahl, M. *Rev. Comput. Chem.* **2002**, *3*, 41–87.
- DesJarlais, R. L.; Seibel, G. L.; Kuntz, I. D.; Furth, P. S.; Alvarez, J. C., et al. *Proc. Natl. Acad. Sci. U.S.A.* **1990**, *87*, 6644–6648.
- Grüneberg, S.; Stubbs, M. T.; Klebe, G. *J. Med. Chem.* **2002**, *45*, 3588–3602.
- Schoichet, B. K.; Stroud, R. M.; Santi, D. V.; Kuntz, I. D.; Perry, K. M. *Science* **1993**, *259*, 1445–1450.
- Foloppe, N.; Chen, I.; Davis, B.; Hold, A.; Morley, D., et al. *Bioorg. Med. Chem.* **2004**, *12*, 935–947.
- Knowles, D. *Curr. Drug Discovery* **2002**, *31*–35.
- Baurin, N.; Baker, R.; Richardson, C.; Chen, I.; Foloppe, N., et al. *J. Chem. Inf. Comput. Sci.* **2004**, *44*, 643–651.
- Foloppe, N.; Fisher, L. M.; Francis, G.; Howes, R.; Kierstan, P., et al. *Bioorg. Med. Chem.* **2006**, *14*, 1792–1804.
- Hann, M. M.; Leach, A. R.; Harper, G. *J. Chem. Inf. Comput. Sci.* **2001**, *41*, 856–864.
- Oprea, T. I.; Davis, A. M.; Teague, S. J.; Leeson, P. D. *J. Chem. Inf. Comput. Sci.* **2001**, *41*, 1308–1315.
- Lipinski, C. A.; Lombardo, F.; Dominy, B. W.; Feeney, P. J. *Adv. Drug Delivery Rev.* **1997**, *23*, 3–25.
- Charifson, P. S.; Walters, W. P. *J. Comput. Aided Mol. Des.* **2002**, *16*, 311–323.
- Rishton, G. M. *Drug Discovery Today* **2003**, *8*, 86–96.
- Morley, S. D.; Afshar, M. *J. Comput. Aided Mol. Des.* **2004**, *18*, 189–208.
- Morley, D. in preparation.
- <<http://www.chemcomp.com/>>.
- Jones, G.; Willett, P.; Glen, R. C. *J. Comput. Aided Mol. Des.* **1995**, *9*, 532–549.

50. Labute, P.; Williams, C. J. *J. Med. Chem.* **2001**, *44*, 1483–1490.
51. Sheridan, R. P.; Kearsley, S. K. *Drug Discovery Today* **2002**, *7*, 903–911.
52. Lengauer, T.; Lemmen, C.; Rarey, M.; Zimmermann, M. *Drug Discovery Today* **2004**, *1*, 27–34.
53. Noble, M. E.; Endicott, J. A.; Johnson, L. N. *Science* **2004**, *303*, 1800–1805.
54. Polgár, T.; Baki, A.; Szendrei, G. I.; Keseru, G. M. *J. Med. Chem.* **2005**, *48*, 7946–7959.
55. Steiner, T. *New J. Chem.* **1998**, 1099–1103.
56. Pierce, A. C.; Sandretto, K. L.; Bemis, G. W. *Proteins* **2002**, *49*, 567–576.
57. Merlot, C.; Domine, D.; Cleva, C.; Church, D. J. *Drug Discovery Today* **2003**, *8*, 594–602.
58. Wildman, S. A.; Crippen, G. M. *J. Chem. Inf. Comput. Sci.* **1999**, *39*, 868–873.
59. Russom, C. L.; Bradbury, S. P.; Broderius, S. J.; Hammermeister, D. E.; Drummond, R. A. *Environ. Toxicol. Chem.* **1997**, *16*, 948–967.
60. Agrawal, V. K.; Khadikar, P. V. *Bioorg. Med. Chem.* **2001**, *9*, 3035–3040.
61. Kalgutkar, A. S.; Gardner, I.; Obach, R. S.; Shaffer, C. L.; Callegari, E., et al. *Curr. Drug Metab.* **2005**, *6*, 161–255.
62. Toledo, L. M.; Lydon, N. B.; Elbaum, D. *Curr. Med. Chem.* **1999**, *6*, 775–805.
63. Williams, D. H.; Mitchell, T. *Curr. Opin. Pharmacol.* **2002**, *2*, 567–573.
64. Chen, P.; Gatei, M.; O'Connell, M. J.; Khanna, K. K.; Bugg, S. J., et al. *Oncogene* **1999**, *18*, 249–256.
65. Greenwood, D. *Antimicrobial Chemotherapy*; Oxford University Press: Oxford, 2000.
66. Stahl, M.; Bohm, H. J. *J. Mol. Graph. Mod.* **1998**, *16*, 121–132.
67. Bridges, A. J. *Chem. Rev.* **2001**, *101*, 2541–2571.
68. Scapin, G. *Drug Discovery Today* **2002**, *7*, 601–611.
69. Jones, G.; Willett, P.; Glen, R. C. *J. Mol. Biol.* **1995**, *245*, 43–53.
70. Kramer, B.; Rarey, M.; Lengauer, T. *Proteins* **1999**, *37*, 228–241.
71. Friesner, R. A.; Banks, J. L.; Murphy, R. B.; Halgren, T. A.; Klicic, J. J., et al. *J. Med. Chem.* **2004**, *47*, 1739–1749.
72. Nissink, J. W. M.; Myrray, C.; Hartshorn, M.; Verdonk, M. L.; Cole, J. C., et al. *Proteins* **2002**, *49*, 457–471.
73. Perola, E.; Charifson, P. S. *J. Med. Chem.* **2004**, *47*, 2499–2510.
74. Hünenberger, P. H.; Helms, V.; Narayana, N.; Taylor, S. S.; McCammon, J. A. *Biochemistry* **1999**, *38*, 2358–2366.
75. Davis, A. M.; Teague, S. J. *Angew. Chem. Int. Ed.* **1999**, *38*, 736–749.
76. Gasteiger, J.; Rudolph, C.; Sadowski, J. *Tetrahedron Comput. Methodol.* **1990**, *3*, 537–547.
77. Berman, H. M.; Westbrook, J.; Feng, Z.; Gilliland, G.; Bhat, T. N., et al. *Nucleic Acids Res.* **2000**, *28*, 235–242.
78. MacKerell, A. D., Jr.; Bashford, D.; Bellott, M.; Dunbrack, R. L., Jr.; Evanseck, J. D., et al. *J. Phys. Chem. B* **1998**, *102*, 3586–3616.
79. Halgren, T. J. *Comput. Chem.* **1996**, *17*, 490–519.
80. <<http://www.asinex.com/>>.
81. <<http://www.ibscreen.com/>>.
82. <<http://www.chemdiv.com/>>.
83. <<http://www.chembridge.com/>>.